Supporting Information

McNaughton et al. 10.1073/pnas.1009648107

SI Text

Supplementary Spectroscopic Results. Continuous Wave EPR spectra of all the yeast strains, taken at X (9 GHz), Q (35 GHz), and W (95 GHz) bands and electron spin echo (ESE) EPR spectra at 35 GHz all show intense signals from low molecular weight Mn^{2+} ($S = 5/2$) that overwhelm any signals from other paramagnetic centers (e.g., Fe centers) in the cell. Unfortunately we find that EPR spectroscopy is not sensitive to the speciation of cellular Mn^{2+}, showing only small, uninterpretable differences among phosphates standards and yeast strains (Fig. S1).

In contrast, 35 GHz Davies pulsed electron-nuclear double resonance (ENDOR) (1) spectra reveal details of Mn^{2+} speciation in viable yeast cells. Fig. S2 displays the ENDOR spectra of wild-type (WT) yeast cells along with those of Mn^{2+} in aqueous solution and in the presence of saturating amounts of Pi and pP, and Fig. 1 shows spectra of the mutant yeast strains. ENDOR of a paramagnetic metal-ion center such as Mn^{2+} provides an NMR spectrum of the nuclei that is hyperfine-coupled to the electron spin (2), and thus can be used to identify and characterize coordinating ligands (3, 4). The frozen-solution spectrum of an $I = 1/2$ nucleus, such as ^{31}P and ^{1}H, coupled to Mn^{2+} comprises a set of doublet features centered at the nuclear Larmor frequency and split by multiples of the electron-nuclear hyperfine coupling (A). The primary doublet is associated with the $m_s = \pm 1/2$ spin electron spin sublevels of Mn^{2+} and is split by A; weaker satellite doublets associated with the $m_s = \pm 3/2$ and $\pm 5/2$ sublevels are split by $3A$ and $5A$ (5). All spectra in this study display ^{1}H signals that can be assigned to the protons of bound water (6). In addition, all the spectra, except for the aqueous solution, show a sharp $m_s = \pm 1/2$ ^{31}P doublet from a phosphate moiety bound to Mn^{2+} center.

The intensities of ^{31}P and ^{1}H signals differ significantly among the spectra so analysis of these intensities can provide a means of assessing Mn^{2+} speciation and its variation with changes in homeostasis. As noted in the text, integrations of ENDOR peaks and measurements of peak intensities give equivalent results. For this initial study the Davies pulsed ENDOR responses have been quantified by measuring the intensities of the ^{1}H and ^{31}P features indicated in Figs. 1 and 2, and they have been used to define the absolute pulsed ENDOR responses, denoted $^{31}P\%$ and $^{1}H\%$, as the fractional changes in the ESE associated with the ^{31}P and ^{1}H ENDOR signals (x 10); direct comparison shows that simple use of intensities gives the same result as using the integrated peaks. The resulting values for the yeast strains are collected in Table 2 and are plotted in Fig. 2 as a function of the analytically derived total orthophosphate concentration, [Pi] (Table 1). To obtain a more detailed picture of Mn^{2+} speciation in whole cells we have developed a protocol for decomposing the observed ENDOR spectra into the contributions from the major Mn^{2+} coordination complexes that are present (see below).

Analysis of Manganese Ligand Binding and Speciation. The decompositions of spectra from cells through use of Eq. **1** require values for the absolute ENDOR responses, N_i (fractional change in the ESE intensity), $N = {}^{1}H$ or ^{31}P, for the reference species, i = hexaaquo (*aq*), Pi-bound (*Pi*), or pP-bound (*pP*) Mn^{2+}. To obtain these, titrations of hexaaquo-Mn^{2+} by L = Pi, Pp were performed, Fig. S3. As can be seen from Fig. S4, the titrations are well-described by Eq. **S1** with $n = 1$ for Pi and $n = 2$ for pP.

$$x_L = \frac{[L]^n}{K_i + [L]^n} \qquad N\%_i = N_i x_L + N_{aq}(1 - x_L). \qquad \textbf{[S1]}$$

The resulting values for the limiting ENDOR responses of the individual reference species, N_i are,

$$\begin{array}{ll} P_{Pi} = 44 & H_{aq} = 44 \\ P_{pP} = 67 & H_{Pi} = 26 \\ & H_{pP} = 10 \\ & H_s = 10 \end{array}$$

Here, in the absence of information about the ENDOR-silent ligands we assumed that $H_s = H_{pP}$. In the decompositions according to the procedures outlined in the text and described in more detail below, we employed the dissociation constants reported by Sigel and coworkers (7) for Pi, $K_{Pi} = 4$ mM and by Van Wazer and coworkers (8) for pP, $K_{pP} = 0.075$ mM. The dissociation constants derived from the present titrations for Pi and pP (Figs. S4, 5) are each tenfold higher due to the influence of the glycerol (or methanol) in the solutions, that is necessary for glassing as required to obtain good ENDOR responses from low molecular weight complexes in solution: $K_{Pi} = 40$ mM and $K_{pP} = 0.75$ mM. Comparison calculations of speciation with the protocol described below show that it is the relative values of the K_L that control the calculated speciation.

For a solution of Mn^{2+} that contains both Pi and pP, competition experiments indicate that Pi and pP binding may be treated as competitive, with negligible formation of mixed-ligand complexes as might be expected from the disparity in binding affinities. In this case, the fraction (y_i) of the Mn^{2+} in the Pi-bound, pP-bound, and hexaaquo forms in an aqueous solution with ligand concentrations, [Pi] and [pP] are given by,

$$\begin{aligned} y_{Pi} &= \frac{K_{pP}[Pi]}{K_{Pi}K_{pP} + K_{pP}[Pi] + K_{Pi}[pP]^2} \\ y_{pP} &= \frac{K_{Pi}[pP]^2}{K_{Pi}K_{pP} + K_{pP}[Pi] + K_{Pi}[pP]^2} \\ y_{aq} &= 1 - (y_{Pi} + y_{pP}). \end{aligned} \qquad \textbf{[S2]}$$

Cells contain not only Pi and pP, but also ENDOR-silent ligands that bind competitively with the two phosphato ligands to Mn^{2+}, generating a fraction (f_s) of the total Mn^{2+} that contributes to the ESE but is coordinated only by the ENDOR-silent ligands. In this case, the fractions of EPR-active Mn^{2+} in the three ENDOR-active states, denoted f_i for i = aq, Pi, pP, may be written in terms of the y_i and f_s,

$$f_i = y_i(1 - f_s) \qquad i = \text{aq,P}_i\text{,pP}. \qquad \textbf{[S3]}$$

The ^{1}H and ^{31}P ENDOR responses from such a solution may be written either in terms of the y_i and f_s or the f_i,

$$\begin{aligned} {}^{1}H\% &= [H_{Aq}y_{Aq} + H_{Pi}y_{Pi} + H_{pP}y_{pP}](1\text{-}f_s) + H_s f_s \\ &= H_{Aq}f_{Aq} + H_{Pi}f_{Pi} + H_{pP}f_{pP} + H_s f_s \\ {}^{31}P\% &= [P_{Pi}y_{Pi} + P_{pP}y_{pP}](1\text{-}f_s). \end{aligned} \qquad \textbf{[S4]}$$

The second formulation describes the ENDOR responses in terms of the fractional speciation of the Mn^{2+}, the four f_i, whose determination is the goal of a spectrum decomposition. The first formulation highlights the fact that these responses are determined by: (*i*) the fraction of Mn^{2+} bound in ENDOR-active complexes ($1\text{-}f_s$); (*ii*) the Pi and pP concentrations, which determine

the y_i, the distribution of the ENDOR-active Mn^{2+} ions among the three contributing forms.

When the two speciation equations of Eq. **1** are formulated in terms of the y_i and f_s, as in Eq. **S4**, they in turn function as three variables, [Pi], [pP], and f_s. These equations were programmed in a Mathcad® worksheet to obtain a solution for [pP] and f_s for each sample from the ENDOR-measured pair of values, ^{31}P% and ^{1}H%, upon assignment of a value for [Pi].

As validation of this heuristic approach, the resulting values for the f_i are shown in Table 2 to be robust to variations of the assigned Pi concentration over a wide range around the [Pi] values measured for each strain. In particular, the key *trends* in speciation caused by mutation-induced changes in Mn^{2+} or phosphates homeostasis are largely insensitive to the assigned [Pi] value, and there are only modest alterations in the ratio, f_{Pi}/f_{pP}. In addition, the effective/average pP concentration obtained in the solution to the speciation equations is found to vary in synchrony with measured pP concentrations (Table 1), providing additional support for the utility of this approach.

SI Materials and Methods. ***Yeast strains, growth conditions, and plasmids.*** All yeast strains in this study were derived from BY4741 (*MATa, leu2Δ0, met15Δ0, ura3Δ0, his3Δ1*) and include the previously reported MC130 strain (*sod1Δ::LEU2 vph1 Δ::kanMX4*) (9), as well as the commercially available *kanMX4* deletion derivatives of *smf2*, *vph1*, *pho85*, and *sod1*, which were all verified by colony purification and gene sequencing. AR167 (*pmr1Δ::LEU2*) and AR168 (*sod1Δ::kanMX4 pmr1Δ::LEU2*) were obtained by deleting *PMR1* from the BY4741 parent strain and the *sod1Δ::kanMX4* strain as described (10). AR169 (*smf2Δ::kanMX4 sod1Δ::LEU2*) and AR030 (*pho85Δ::kanMX4 sod1Δ::LEU2*) were obtained by deleting *SOD1* from the *smf2Δ::kanMX4* and *pho85Δ::kanMX4* strains as described previously (11).

All experiments employed cells freshly obtained from frozen stocks and cultured on enriched yeast extract, peptone, dextrose medium (YPD) at 30 °C (12). Experiments involving *sod1Δ* mutants were precultured anaerobically on YPD media supplemented with 15 mg/L ergosterol and 0.5% Tween 80 (YPDE), and grown at 30 °C in anaerobic chambers (GasPak, Becton-Dickinson).

For EPR/ENDOR analysis of yeast cells, cultures were inoculated at a starting $OD_{600} = 0.05$ in 25 mL of YPD in a 250 mL Erlenmeyer flask and grown overnight shaking at 220 rpm and 30 °C until they reached a final $OD_{600} = 2.0$. The cultures were pelleted by centrifugation and washed three times with ice-cold MiliQ purified water. $\sim 2 \times 10^9$ cells/mL was resuspended in 30% Glycerol/50 mM Hepes Buffer/ pH = 7.0 and added to an EPR tube and flash frozen in an ethanol/dry ice bath.

To assay for oxygen sensitivity, 10^4, 10^3, and 10^2 cells of various yeast strains were spotted onto YPDE plates and allowed to grow at 0%, 10%, 20%, and 40% O_2, balance N_2, for 3 d. The various oxygen tensions were achieved by placing the YPDE plated cells in an anaerobic chamber (Vacu-Quik Jar, Almore), which was then subjected to five cycles of vacuum and gas filling. The appropriate O_2/N_2 mixes were achieved by using a high precision (±1%) gas mixer (KM 20-2, WITT GAS) connected to O_2 and N_2 gas cylinders.

Biochemical assays. To determine the manganese content of the various yeast strains, atomic absorption spectroscopy analysis of whole cells was carried out on a PerkinElmer Life Sciences AAnalyst 600 graphite furnace atomic absorption spectrometer according to the manufacturer's specifications, as described previously (9).

Phosphate content of whole cell lysates was determined using the colorimetric molybdate assay (13, 14). Prior to phosphate analysis, the cells were grown and washed as described above for the EPR/ENDOR analysis, resuspended in 500 μL 0.1% Triton X-100, and lysed by glass bead homogenization. Protein content of the lysates was determined by using a BioRad Protein Assay kit according to the manufacturer's specifications. Total phosphate was measured from boiling 3–30 μg of whole cell lysates for 10 min in 1 Normal H_2SO_4. Orthophosphate was measured from unboiled samples. Polyphosphate is taken as the difference between the boiled and unboiled samples (13, 14).

Preparation of aqueous Mn^{2+} standard samples. A series of standard solutions for ENDOR analysis containing 100 μM $MnCl_2$ and either phosphate or polyphosphates at varied concentrations were prepared. All solutions contained 20% glycerol as glassing agent; equivalent results were obtained when methanol was used as glassing agent. Final pH of the Mn-phosphate standards was ~7 while the polyphosphates standards were adjusted to a slightly more acidic pH of ~6.5 to mimic the luminal environment of the vacuole where the bulk of the cell's polyphosphates are stored. Since the polyphosphates used in the preparation of the standards varied in length ($Na_{15}P_{13}O_{40} - Na_{20}P_{18}O_{55}$), the molar quantities were not exact; calculations for the polyphosphates standards were performed using the median formula weight.

EPR and electron-nuclear double resonance measurements.

Spectroscopy:

35 GHz pulsed EPR and ENDOR spectra were obtained using a laboratory-built spectrometer (15) equipped with a helium immersion dewar for measurements at ~2 K and a solid-state 4W microwave amplifier (Microwave Power Inc.). Data acquisition utilized the SpecMan software package (16) with a 400 MHz word generator (Spin-Core PulseBlaster ESR_PRO) and a 500 MS/sec digitizer (Agilent Technologies Acquiris DP235). ESE EPR spectra were obtained using a two-pulse Hahn sequence ($tp - \tau - 2tp - \tau -$ echo), producing an absorption-mode spectrum that displays all of the $|\Delta M_S| = 1$ transitions. All ENDOR spectra were obtained using a Davies pulse sequence (tp-T-$tp/2$-τ-tp-τ-echo) where the rf was applied during interval T (1). Frequencies within the rf range chosen for the spectrum were accessed randomly (stochastic ENDOR). Signal averaging was accomplished by collecting multiples of such spectra rather than by multiple acquisitions at each frequency (17), and broadening of the rf to 100 kHz was used to improve signal-to-noise (18).

W-band (95 GHz) CW EPR spectra were collected at ~140 K with a laboratory-designed homodyne bridge assembled by Millitech Corp., to be described elsewhere, with 100 kHz field modulation as the detection scheme.

Electron-nuclear double resonance quantitations:

Each ENDOR spectrum was collected over the 10–80 MHz frequency range as the average of at least 50 samplings per randomly accessed frequency point. The magnetic field was set to correspond to the resolved ^{55}Mn hyperfine line at lowest field. The baseline of the ENDOR spectra was corrected linearly when necessary using the high-frequency region as the zero intensity. Several quantitation methods were tested to determine the most consistent and reliable measure of the ^{31}P and ^{1}H ENDOR intensities across samples and relative to each other, including: separate data collection in the ^{31}P and ^{1}H regions; integration of the $\pm 1/2$ peaks; integration of all ^{31}P/^{1}H peaks; and maximum intensity at a selected ENDOR peak. We found that the ν_+ ^{31}P peak (see Fig. 1) does not vary in breadth among phosphate standards or yeast strains, and its intensity provided the most convenient and reproducible measure of ^{31}P intensity. The less convenient method of integrating ^{31}P peaks also was less reliable because of baseline variability below ~20 MHz that is known to occur for ENDOR spectra of Mn^{2+} complexes when the concentration of Mn is high (6). As noted in the text, we have been and

are exploring different methods of quantitating the ^{1}H signal, including measurement of the intensity of individual resolved features and integration of all or part of the ^{1}H pattern. However, we find that the sharp feature indicated in Fig. 1, like the chosen ^{31}P peak, does not vary in width from sample to sample, and that the simple procedure, analogous to that for ^{31}P, of measuring its intensity, robustly describes the behavior of multiple standards samples and multiples of each of the variants. To calculate the % ENDOR response value, the measured ^{31}P or ^{1}H peak intensity (in volts) is scaled by the maximum ESE intensity (volts) for that sample, measured using the two-pulse Hahn sequence described above, at the identical magnetic field that the ENDOR spectrum was collected. The ESE intensity was measured as the difference in the ESE maximum at that field to the response at zero applied field (the most reliable "off resonance field" because the EPR spectrum of Mn^{2+} is so broad, Fig. S1).

1. Schweiger A, Jeschke G (2001) *Principles of pulse electron paramagnetic resonance* (Oxford University Press, Oxford, United Kingdom).
2. Abragam A, Bleaney B (1970) *Electron paramagnetic resonance of transition ions* (Clarendon Press, Oxford).
3. Hoffman BM (2003) ENDOR of metalloenzymes. *Acc. Chem. Res.* 36:522–529.
4. Hoffman B (2003) ENDOR (and ESEEM) in bioinorganic chemistry. *Proc. Natl. Acad. Sci. USA* 100:3575–3578.
5. Potapov A, Goldfarb D (2006) Quantitative characterization of the Mn^{2+} complexes of ADP and ATPgS by W-band ENDOR. *Appl. Magn. Res.* 30:461–472.
6. Sivaraja M, Stouch TR, Dismukes GC (1992) Solvent structure around cations determined by proton ENDOR spectroscopy and molecular dynamics simulation. *J. Am. Chem. Soc.* 114:9600–9603.
7. Saha A, et al. (1996) Stability of metal-ion complexes formed with methyl phosphate and hydrogen phosphate. *J. Biol. Inorg. Chem.* 1:231–238.
8. Van Wazer JR, Campanella DA (1950) Structure and properties of the condensed phosphates. IV. Complex-ion formation in polyphosphate solutions. *J. Am. Chem. Soc.* 72:655–663.
9. Reddi AR, et al. (2009) The overlapping roles of manganese and Cu/Zn SOD in oxidative stress protection. *Free Radical Biol. Med.* 46:154–162.
10. Lapinskas PJ, Cunningham KW, Liu XF, Fink GR, Culotta VC (1995) Mutations in PMR1 suppress oxidative damage in yeast cells lacking superoxide dismutase. *Mol. Cell. Biol.* 15:1382–1388.
11. Culotta VC, Joh H-D, Lin S-J, Slekar KH, Strain J (1995) A physiological role for *Saccharomyces cerevisiae* copper/zinc superoxide dismutase in copper buffering. *J. Biol. Chem.* 270:29991–29997.
12. Sherman F, Fink GR, Lawrence CW (1978) *Methods in yeast genetics* (Cold Spring Harbor Laboratory Press, Cold Spring Harbor, New York).
13. Ames BN (1966) *Methods enzymol.*, eds. Neufeld, E, Ginsburg V (Academic Press, New York, New York), Vol. VIII: Complex Carbohydrates, 115–118.
14. Kulaev IS, Vagabov V, Kulakovskaya T (2004) *Biochemistry of inorganic polyphosphates*, 2nd Ed. (John Wiley and Sons, Ltd, West Sussex, England).
15. Davoust CE, Doan PE, Hoffman BM (1996) Q-band pulsed electron spin-echo spectrometer and its application to ENDOR and ESEEM. *J. Magn. Reson.* 119:38–44.
16. Epel B, Gromov I, Stoll S, Schweiger A, Goldfarb D (2005) Spectrometer manager: a versatile control software for pulse EPR spectrometers. *Concepts in Magnetic Resonance Part B: Magnetic Resonance Engineering* 26B:36–45.
17. Epel B, Arieli D, Baute D, Goldfarb D (2003) Improving W-band pulsed ENDOR sensitivity—random acquisition and pulsed special TRIPLE. *J. Magn. Reson.* 164:78–83.
18. Hoffman BM, DeRose VJ, Ong JL, Davoust CE (1994) Sensitivity enhancement in field-modulated CW ENDOR via RF bandwidth broadening. *J. Magn. Reson.* 110:52–57.

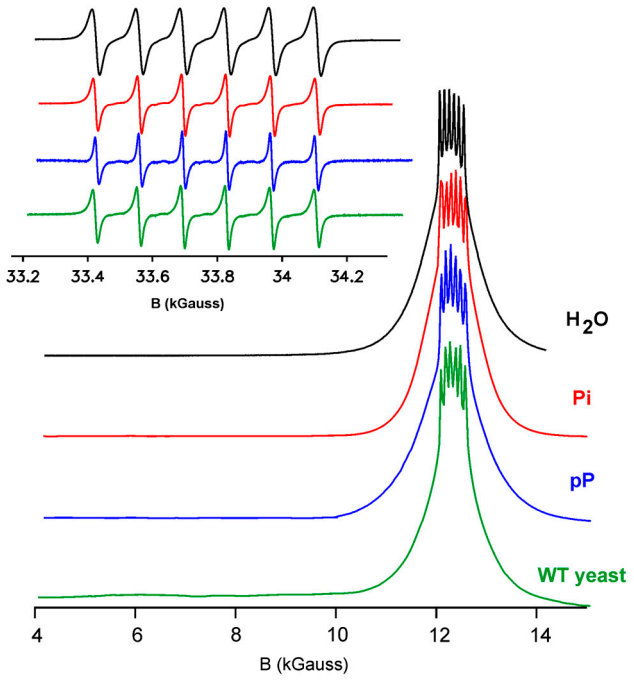

Fig. S1. Q-band pulsed and W-band CW EPR spectra of Mn^{2+} standards and WT yeast cells. All spectra show the six-line pattern characteristic of hyperfine coupling to the ^{55}Mn ($I = 5/2$) nucleus associated with the $m_s = \pm 1/2$ electron spin ($S = 5/2$) sublevels, plus intensity spreading over several thousand Gauss associated with the $m_s = \pm 3/2, \pm 5/2$ sublevels. *Conditions:* Q-band pulsed, $T = 2$ K, $tp = 60$ ns, $\tau = 700$ ns, repetition time = 20 ms. W-band CW, $T = 140$ K, modulation amplitude = 2 G.

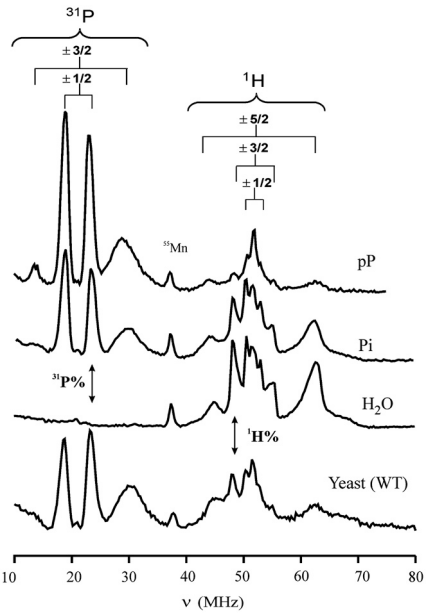

Fig. S2. 35 GHz Davies pulsed ENDOR spectra of Mn^{2+} standards plus that from viable WT yeast cells, with the ^{1}H and ^{31}P features from the individual Mn^{2+} ($S = 5/2$) substates indicated. "Mn" corresponds to the third harmonic of a ^{55}Mn transition that was not filtered out, leaving a fiduciary mark. The double-headed arrows indicate the features used to quantitate the ENDOR intensities. *Conditions:* $T = 2$ K, MW pulse = 60 ns, $\tau = 700$ ns, RF pulse = 40 μs, repetition time = 20 ms.

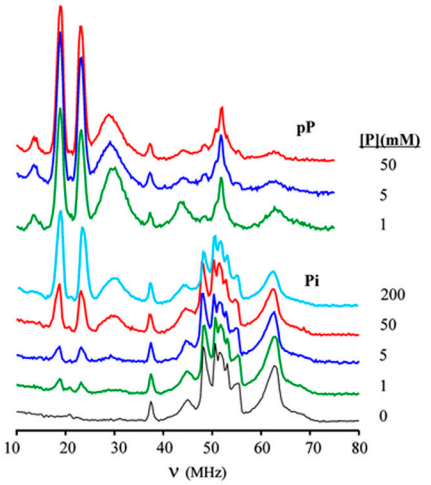

Fig. S3. Selected 35 GHz pulsed ENDOR spectra collected during titrations of aqueous Mn^{2+} with Pi and pP. *Conditions:* As in Fig. S2.

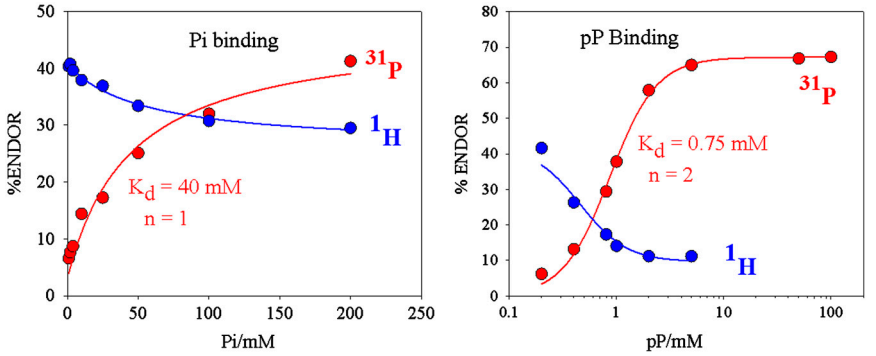

Fig. S4. Plots of $^{31}P\%$ and $^{1}H\%$ measured during titrations of aqueous Mn^{2+} with Pi *(left)* and pP *(right)*. Solid lines are fits to Eq. **S1** for $n = 1$ (Pi) and $n = 2$ (pP).